Title

Acceleration of *Drosophila subobscura* evolutionary response to global warming in Europe

Author list

Francisco Rodríguez-Trelles, Rosa Tarrío

Affiliations

Departament de Genètica i de Microbiologia, Facultat de Biociències, Universitat Autonòma de Barcelona, 08193 Bellaterra (Barcelona), Spain.

Corresponding author's email: franciscojose.rodrigueztrelles@uab.cat

Abstract

The increasing risk of irreversible ecological transformation under global warming has boosted the need to understand the capacity of organisms to adapt to this change. Here, using a resurvey method of populations of the European fly *Drosophila subobscura*, we show that a known evolutionary response to global warming has accelerated in the last 20 years, in step with regional warming. This genetic response has come entirely by resorting pre-existing variation – and not from novel inversions – for tolerance to high temperature. Temperate populations are predicted to converge to the typical Mediterranean chromosomal composition by the mid-2050s, at which point this classic example of steep genetic cline will have vanished. Our results suggest species with broad geographic ranges, large population sizes, and high genetic diversity may have the evolutionary potential to cope with climate change.

Main text

Main

The biological impacts of human-caused global warming are worsening as predicted[1,2,3]. Early studies concentrated on detecting ecological and evolutionary signals of warming impacts[4,5]. Subsequently, studies have followed the progression of these changes. Evolutionary adaptation is a significant form of resilience to global warming, as it may be the only way for a population to survive when nongenetic compensatory responses are exceeded by environmental change[6,7,8]. Given the geographic and chronological progression of the global temperature increase, it is crucial to understand if the observed changes are sufficient to enable populations to adapt[9,10,11,12].

Early evolutionary impacts of global warming were detected in the widespread temperate fly *Drosophila subobscura*[13,14]. This species has a rich chromosomal inversion polymorphism distributed over its five major chromosomes (denoted by the letters A, J, U, E and O). Inversions are large-scale structural mutations (spanning tens, hundreds, or more genes) that involve breakage and reversal of a chromosomal segment, resulting in new variants of gene arrangements[15,16,17,18]. Inversions limit recombination and may result in linked sets of co-adapted alleles to local environmental conditions. In *D. subobscura*, structurally segregating regions collectively account for ~ 83% of the species' genome, meaning that the fraction of genetic loci unaffected by rearrangements is comparatively small[19,20].

Past comprehensive summaries of the species' abundant inversion polymorphism revealed that the gene arrangements from more equatorial Palearctic populations are gradually replaced by the so-called Standard gene arrangements in the five chromosomes as populations approach high latitudes[19]. Similar clinal patterns became independently established in North and South America following the species' recent spread in both continents[21]. In accordance with the clinal patterns, Standard gene arrangements undergo regular seasonal cycles increasing during winter and decreasing during summer repeatedly over the years[22,23]. Taken together, these findings suggested an adaptive relationship between inversion frequencies and climate[13,24].

Based on this, Balanyá *et al*.[14] compared within-site shifts in inversion frequencies over a broad latitudinal scale from pre-global warming to the late 1990s. They found that the frequencies of low-latitude (putatively warm-adapted) inversions increased with the magnitude of global warming between sample periods. Here we update those early findings by resurveying European populations twenty years later using the same methods as Balanya *et al*.[14]. Our findings corroborate that anthropogenic global warming is continuing to shift the genetic composition of this species, and show that novel patterns are emerging.

Follow-up survey of the early evolutionary warning

Earlier data on genetic response of *D. subobscura* to contemporary global warming in Europe were drawn from ref.[14]. They consisted of historical survey ("HS") and resurvey ("R1") records from 12 main continental sites distributed across seven countries, comprising Austria (Vienna [VN]), Belgium (Louvain-la-Neuve [LN]), France (Lagrasse [LG], Montpellier [MP] and Villars [VL]), Germany (Tübingen [TB]), the Netherlands (Groningen [GN]), Spain (Málaga [ML], Punta Umbría [PU], Riba-roja de Túria [RT] and Queralbs [QR]), and Switzerland (Leuk [LK]) (Fig. 1). The sample spans a 16.5º latitude range that is split into two climatic regions: Mediterranean to the south (ML, PU, RT, QR, LG, and MP) and temperate to the north (VL, LK, VN, TB, LN, and GN). The HS record was collected around the end of the 1960s (1968 ± 7.3 years), prior to recent warming, whereas the R1 record was collected at the end of 1990s (1999 ±

1.4 years). Almost two decades later (2017 ± 1.5 years), we conducted a new resurvey ("R2") at the same sites around the same dates of the year and updated inversion frequencies (Methods; Supplementary Table 1[27]). The aggregated records span half a century (49.2 ± 7.3 years), with the average elapsed time between R1 and R2 (18.4 ± 2.2 years) being one decade shorter than that between HS and R1 (30.8 ± 7.2 years).

All five chromosomes of the species were examined in each of the 12 samples following standard procedures (*e.g.*, ref.[14]) (Methods). A total of 6,670 chromosomes were scored for gene arrangements (the sample sizes [*N*] for each site and chromosome of the species' five chromosome set are provided in Supplementary Table 1[27]). No newly discovered, previously unreported inversions were detected. Altogether, we used 45 different gene arrangements (Methods).

Shifts in overall average ambient temperature and population genetic composition were assessed using the same temperature (T_{PC1}) and genome-wide chromosome (Ch_{PC1}) indices as in ref.[14]. The two metrics are first principal components of centered unscaled Principal Component Analyses on temperature and genetic data, respectively (Methods). Higher scores between sample periods indicate, in the case of T_{PC1}, increased warming of environmental temperatures, and in the case of Ch_{PC1}, increased frequency of warm-latitude chromosome arrangements.

Faster warming, faster genetic change

T_{PC1} scores are inversely correlated with latitude in all three surveys (Table 1). The relationship is best described by two-segment piecewise linear regression models with a breakpoint at approximately 46.3º, and the piecewise model fit the data better than either unsegmented linear models or second-order polynomial models (Fig. 2A; Supplementary Tables 2 and 3). This breakpoint should not be taken as an absolute value but rather as a transition zone between Mediterranean and temperate western Europe (Supplementary Table 4). Although warming has continued since R1 (Fig. 3; Wilcoxon tests; Supplementary Table 5), warming has been faster at the temperate sites (Fig. 3; Mann-Whitney U tests; Supplementary Table 5).

Ch_{PC1} scores are inversely correlated with latitude and directly with T_{PC1} in all three surveys (Table 1, Fig. 2, B and C). The decline of Ch_{PC1} with latitude and its rise with T_{PC1} are equally well described by two-segment linear functions with a similar breakpoint to that found for T_{PC1} or by second-order polynomial functions (compared to unsegmented linear baselines) (Fig. 2, B and C; Supplementary Table 2, 3 and 6). The smoothness of the genetic change when compared to the temperature change across the Mediterranean-temperate transition is probably a reflection of the mixing of flies across sites. No significant spatial autocorrelation is found in the residuals after fitting the T_{PC1} (second-order polynomial) model (Moran's I = -0.18, -0.15, and -0.12; for HS, R1 and R2, respectively; expected Moran's I = ~ -0.09 and Monte Carlo $P > 0.3$ in all cases). Thus, inversion frequencies shift latitudinally as if driven by the local climate. Likewise, if the observed temporal patterns of magnitudes of climate change had a genetic impact, then Ch_{PC1} should also reflect this relationship. In fact, Ch_{PC1} not only has continued increasing since R1 (Wilcoxon tests; Supplementary Table 5), but has done so at an accelerated rate at the temperate sites, in step with T_{PC1} (Fig. 3; Mann-Whitney U tests; Supplementary Table 5). Both the discontinuity in the latitudinal thermal gradient and the acceleration in the rate of evolutionary response correlative to climate warming are not described in the previous study.

The observed geographic heterogeneity in the timing of the genetic shift suggests that it is due in part to local adaptation rather than just to genetic drift or a northern migration of individuals from equatorial locations. Genetic drift is not likely a factor, considering the large-scale of the

phenomenon (multiple populations shifting in the same direction across a wide geographic range). On the other hand, if migration was responsible, frequencies of some sporadic inversions that are relatively common in North Africa (e.g., A_{2+6} and $E_{1+2+9+4}$) should have also increased in southern Europe; but this was not observed. Local adaptation is further supported by the fact that the individual contributions of each of the species' five chromosomes to the acceleration of the shift at the temperate sites have not been homogeneous (Fig. 3), despite the fact that they started from similar levels of latitudinal differentiation in R1 [ref.[14]; Supplementary Table 1[27]]. The observed inter-chromosomal variation in evolutionary rate rather suggests that chromosomes differ in their effects on the thermal phenotype.

Association with extreme heat

The T_{PC1} patterns observed in the present study align with reported geographic and temporal trends in the frequency and magnitude of heatwaves in Europe[29,30]. Specifically, the rate of incidence and duration of major European heatwaves increased continent-wide from the first sample interval (HS-R1) to the second (R1-R2), but those shifts were approximately twice as high in central Europe (14 events, aggregating 223 days in length) as in southern Europe (8.0 events, 104 days) or in Southwest Europe (6.0 events, 90 days)[30]. The results of this latest study[30] allowed us to obtain a raw estimate of the degree of heat wave exposure, hereon referred to as *HWe*, individually for each sample site (Methods; Fig. 4). The decadal rates of *HWe* increased from HS-R1 to R1-R2 at all sites (P = < 1× 10-3, one-tailed exact Wilcoxon signed rank test, n = 12), but the rate of increase was faster at the temperate than at the Mediterranean sites (P = 0.002, two-tailed exact independent samples Mann-Whitney U test, n = 6). A significant positive association between the decadal rates of Ch_{PC1} and *HWe* emerged from HS-R1 (two-tailed Spearman's $\rho = 0.387$, P = 0.213, n = 12) to R1-R2 (two-tailed Spearman's $\rho = 0.664$, P = 0.018, n = 12), as would be expected if inversion frequencies were impacted by the rise in major heat waves. In line with our findings, a heatwave caused a surge in the frequency of more thermotolerant genotypes in *D. subobscura* in another study[23]. Therefore, the acceleration in the *D. subobscura* rate of evolutionary response observed in the present study is likely driven not only by the gradual increase in average temperatures, but also more frequent and longer duration heatwaves[31,32,33,34].

The build-up of the association between Ch_{PC1} and *HWe* in the R1-R2 interval could be due to a differential effect of the increase in high- and low-temperature extremes. To investigate this, we developed two analogous indices to T_{PC1} based on the monthly maxima and minima of daily temperatures, respectively referred to as TXx_{PC1} and TNn_{PC1} (Methods). The index better accounting for the chromosome data shifted from extreme minimum in the HS survey (AICc-Wt = 0.96) to extreme maximum in the R2 survey (AICc-Wt = 1.00) (Supplementary Table 8; Supplementary Figure 1). This suggests that a likely factor in the emergence of the association of Ch_{PC1} with *HWe* during the R1-R2 interval was heat wave-imposed selection against the upper thermal tolerance of cold-climate arrangements. This conclusion would agree with laboratory experiments showing that carriers of cold-climate gene arrangements were less heat-stress tolerant than carriers of warm-climate gene arrangements[35]. Note that these experiments were conducted on adults, while inversion-differential effects may be particularly significant for preadult life stages, such as eggs, larvae and pupae, thought to be more vulnerable to heat stress[36].

Discussion

We demonstrated that evolutionary responses to global warming of European *D. subobscura* have not only been rapid, but has accelerated in step with the rise in temperature. These continental responses in Europe seem to be due to local shifts in frequencies of existing (prior to the onset of warming) chromosomal arrangements rather than to the evolution of novel arrangements (or influx from migration from North Africa)[37,38]. Specifically, no novel chromosome inversions have been found (ref.[14]; Supplementary Table 1[27]) despite five decades of climate warming.

Whether the standing chromosomal variation of *D. subobscura* will withstand future warming remains to be determined[3,28,34]. However, if we project current trends, temperate populations are predicted to converge to typical Mediterranean Ch_{PC1} values around the mid-2050s (Fig. 5). At that point the steep genetic cline of this species – a classic in evolutionary genetics – will have vanished. Continued depletion of the pool of inversion variation should make the persistence of *D. subobscura* populations increasingly dependent on the much slower process of emergence of new adaptive mutations[39,40]. Along this path, the ability of the species to genetically track climate change may be enhanced if population connectivity and gene flow is maintained. On the other hand, it could be offset by a range of factors, such as linked deleterious variation[41], trade-offs with other fitness traits[42], mismatched species interactions[43], and effects of other stresses[44]. The already observed decline in the frequency of cold-climate inversions should induce a rapidly co-evolved reduction in cold tolerance[45,46,47,48]. If it persists, this reduction might progressively hamper population's ability to survive sudden reversals of warming trends.

Understanding the precise mechanisms whereby inversions confer adaptation to climate change requires knowledge of the number, identity and relative significance of the genetic loci involved, as well as the specific behavioral, life-history and physiological traits affected by them[49]. Progress has been hampered by the challenges inherent to analyzing inversions[50], particularly in a species like *D. subobscura* that combines overlapping and non-overlapping inversions of variable ages, sizes and positions along every chromosome[19,20]. So far 11 climate-associated inversions have been analyzed at DNA sequence level (*A2*, *U1*, *U2*, *E1*, *E2*, *E9*, *E12*, *O3*, *O4*, *O7*, and *O8*). In all but one case (O_7) the breakpoints are located away from any known gene for climate adaptation[51]. Thus, rather than direct chromosomal breakage, the primary mechanism by which inversions contribute to this species' adaptation to climate change seems to be indirect (via their recombination suppression effect holding together favorable combinations of alleles at climate-adaptive genes), but more research is needed. The prevalence of climate-associated inversions in the genome of *D. subobscura* indicates that the specie's response to global warming is likely a complex multi-trait phenotype.

Continued resurveying of genetic trait frequencies is a powerful means to assess whether evolution will be important under climate change[12]. The results presented herein suggest that the species most able of evolutionary adaptation to anthropogenic climate warming are those with wide-ranges, large population sizes and amounts of genetic diversity. For other species, the ability to adapt through evolution to the changing climate is probably lower[44,52]. It should be noted, however, that just as important as having a high level of genetic diversity is its availability wherever it may be adaptive. As the case of *D. subobscura* might illustrate, certain inversions from North Africa, which could be advantageous in the newly warmer environments of Europe, nevertheless have not spread there. This is probably because, alongside with warm-adaptive alleles, they locked up others with antagonistic effects outside the local environment in which the inversion evolved. The acceleration of the evolutionary impact of human-caused global warming reported here and elsewhere[3,53,54,55,56] increases the urgency for effective mitigation actions.

209

Acknowledgments

We express our special gratitude to Raymond B. Huey, Camille Parmesan, and Mark C. Urban for their critical reading and insightful comments on the manuscript. We gratefully acknowledge the financial support from the Ministerio de Ciencia e Innovación (PID2020-116789, RB-C43, and CGL2017-89160P), Spanish Ministerio de Economía y Competitividad (CGL2013-42432-P), and Generalitat de Catalunya (2021-SGR-00731, and 2017SGR 1379).

Author Contributions

F.R.-T. conceived the study, led the data analysis and the writing of the manuscript with input from RT. The two authors contributed to the survey plan, collection and processing of the samples, and to interpreting the results.

Competing Interests

The authors declare that they have no competing interests.

Tables

Table 1. Two-tailed Spearman's *r* correlation coefficients for the association between chromosome (Ch_{PC1}) and climate (T_{PC1}) indices and latitude for HS, R1 and R2 samples. Confidence intervals (95%) are given in parentheses; all values significant at $P < 0.001$; n = 12.

	HS	R1	R2
T_{PC1} vs Latitude	-0.944 (-0.988, -0.757)	-0.972 (-0.994, -0.870)	-0.958 (-0.991, -0.812)
Ch_{PC1} vs Latitude	-0.937 (-0.987, -0.730)	-0.937 (-0.987, -0.730)	-0.853 (-0.966, -0.466)
Ch_{PC1} vs T_{PC1}	0.930 (0.705, 0.985)	0.972 (0.841, 0.993)	0.902 (0.610, 0.978)

Figure Legends

Fig. 1. The 12 European sample sites and their distribution relative to the Mediterranean-temperate climate transition zone. Black dots indicate the locations of sample sites. The map was built using the *Simplemappr* tool under a Creative Commons license CC0 1.0.[25] using the Mercator projection and the shapefile for the Mediterranean climate region supplied in ref.[26].

Fig. 2. Five decades of *D. subobscura* evolutionary response to global warming in Europe. (a) The PCA-based temperature index T_{PC1} exhibits a two-segment linear piecewise relationship with latitude. The break marks a transition between Mediterranean and temperate western Europe. T_{PC1} increased from HS to R1, and from R1 to R2, but the increase accelerated at the temperate sites over the sample interval R1-R2. (b) The PCA-based chromosome index Ch_{PC1} exhibits a continuous second-order polynomial relationship with latitude, mimicking the patterns of T_{PC1}. (c) Second-order polynomial relationship between Ch_{PC1} and T_{PC1}.

Fig. 3. Decadal rates of equatorialward shift in temperature and inversion frequencies in Europe. T_{PC1}, Ch_{PC1}, and chromosomewise (*i.e.*, for each of the A, J, U, E, and O chromosomes; Methods) indices show greater positive shift rates at temperate sites over the R1-R2 interval, except for the O chromosome. Boxplots show 25–75th percentiles (boxes), medians (center lines), and the minimum-maximum values or, when there are values that are less-more than 1.5 times the interquartile range, the smallest-largest value (whiskers). The numbers below variable names are corresponding exact one-tailed Wilcoxon signed rank test p-values for the null hypothesis of no positive difference between the R1-R2 and HS-R1 sample intervals (n = 6). Chromosomewise p-values < 0.1 per region are considered significant after Benjamini-Hochberg correction for multiple comparisons (false discovery rate set to ≤ 0.1).

Fig. 4. Change in site decadal rate of heat wave exposure (*HWe*) between the two sample intervals. The rate increased from the HS-R1 period to the R1-R2 period at all sites ($P = < 1 \times 10^{-3}$, one-tailed exact Wilcoxon signed rank test, n =12), but the rate increase was faster at the temperate sites (P = 0.002, two-tailed exact independent samples Mann-Whitney U test, n = 6).

Fig. 5. Predicted date when temperate sites will converge on the typical Mediterranean chromosomal composition. The intersection date between the linear ($y = 3.53e^{-3}x + 6.55$) and second-order polynomial ($y = 1.84e^{-4}x^2 + 7.24e^{-1}x + 7.11e^{-2}$) equations is year 2055.03.

References

1. Urban, M. C. Climate change. Accelerating extinction risk from climate change. *Science* **348**, 571–573 (2015).
2. Scheffers, B. R., De Meester, L., Bridge, T. C., Hoffmann, A. A., Pandolfi, J. M., Corlett, R. T., Butchart, S. H., Pearce-Kelly, P., Kovacs, K. M., Dudgeon, D., Pacifici, M., Rondinini, C., Foden, W. B., Martin, T. G., Mora, C., Bickford, D. & Watson, J. E. The broad footprint of climate change from genes to biomes to people. *Science* **354**, aaf7671 (2016).
3. IPCC, 2023: Climate Change 2023: Synthesis Report. Contribution of Working Groups I, II and III to the Sixth Assessment Report of the Intergovernmental Panel on Climate Change [Core Writing Team, H. Lee and J. Romero (eds.)]. IPCC, Geneva, Switzerland, 184 pp.
4. Hughes, L. Biological consequences of global warming: is the signal already apparent?. *Trends. Ecol. Evo.* **15**, 56–61 (2000).
5. Parmesan, C. & Yohe, G. A globally coherent fingerprint of climate change impacts across natural systems. *Nature* **421**, 37–42 (2003).
6. Parmesan, C. Ecological and evolutionary responses to recent climate change. *Annu. Rev. Ecol. Evol. Syst*. **37**, 637–669 (2006).
7. Meester, L. D., Stoks, R. & Brans, K. I. Genetic adaptation as a biological buffer against climate change: Potential and limitations. *Integr*. *Zool*. **13**, 372–391 (2018).
8. Waldvogel, M., Feldmeyer, B., Rolshausen, G., Exposito-Alonso, M., Rellstab, C., Kofler, R., Mock, T., Schmid, K., Schmitt, I., Bataillon, T., Savolainen, O., Bergland, A., Flatt, T., Guillaume, F. & Pfenninger, M. Evolutionary genomics can improve prediction of species' responses to climate change. *Evol*. *Lett*. **14**, 4–18 (2020).
9. Martin, R. A., da Silva, C. R. B., Moore, M. P. & Diamond, S. E. When will a changing climate outpace adaptive evolution? *WIREs Clim*. *Change*. **14**, e852 (2023).
10. Mimura, M., Yahara, T., Faith, D. P., Vázquez-Domínguez, E., Colautti, R. I., Araki, H., Javadi, F., Núñez-Farfán, J., Mori, A. S., Zhou, S., Hollingsworth, P. M., Neaves, L. E., Fukano, Y., Smith, G. F., Sato, Y. I., Tachida, H. & Hendry, A. P. Understanding and monitoring the consequences of human impacts on intraspecific variation. *Evol. Appl*. **10**, 121–139 (2016).
11. Steinbauer, M. J., Grytnes, J.-A., Jurasinski, G., Kulonen, A., Lenoir, J., Pauli, H., Rixen, C., Winkler, M., Bardy-Durchhalter, M., Barni, E., Bjorkman, A. D., Breiner, F. T., Burg, S., Czortek, P., Dawes, M. A., Delimat, A., Dullinger, S., Erschbamer, B., Felde, V. A., Fernández-Arberas, O., Fossheim, K. F., Gómez-García, D., Georges, D., Grindrud, E. T., Haider, S., Haugum, S. V., Henriksen, H., Herreros, M. J., Jaroszewicz, B., Jaroszynska, F., Kanka, R., Kapfer, J., Klanderud, K., Kühn, I., Lamprecht, A., Matteodo, M., di Cella, U. M., Normand, S., Odland, A., Olsen, S. L., Palacio, S., Petey, M., Piscová, V., Sedlakova, B., Steinbauer, K., Stöckli, V., Svenning, J.-C., Teppa, G., Theurillat, J.-P., Vittoz, P., Woodin, S. J., Zimmermann, N. E. & Wipf, S. Accelerated increase in plant species richness on mountain summits is linked to warming. *Nature* **556**, 231–234 (2018).
12. Nadeau, C. P. & Urban, M. C. Eco-evolution on the edge during climate change, *Ecography* **42**, 1280–1297 (2019)

13. Rodríguez-Trelles, F. & Rodríguez, M. Á. Rapid micro-evolution and loss of chromosomal diversity in *Drosophila* in response to climate warming. *Evol. Ecol.* **12**, 829–838 (1998).

14. Balanyà, J., Oller, J. M., Huey, R. B., Gilchrist, G. W. & L. Serra, L. Global genetic change tracks global climate warming in *Drosophila subobscura*. *Science* **313**, 1773–1775 (2006).

15. Kirkpatrick, M. How and why chromosome inversions evolve. *PloS Biol.* **8**, e1000501 (2010).

16. Tigano, A. & Friesen, V. L. Genomics of local adaptation with gene flow. *Mol. Ecol.* **25**, 2144–2164 (2016).

17. Wellenreuther, M. & Bernatchez, L. Eco-evolutionary genomics of chromosomal inversions. *Trends Ecol. Evol.* **33**, 427–440 (2018).

18. Faria, R. Johannesson, K. Butlin, R. K. & Westram, A. M. Evolving inversions. *Trends Ecol. Evol.* **34**, 239–248 (2019).

19. Krimbas, C. B. *Drosophila subobscura: Biology, Genetics and Inversion Polymorphism* (Verlag Dr. Kovac, Hamburg, Germany, 1993).

20. Karageorgiou, C., Gámez-Visairas, V., Tarrío, R. & Rodríguez-Trelles, F. Long-read based assembly and synteny analysis of a reference *Drosophila subobscura* genome reveals signatures of structural evolution driven by inversions recombination-suppression effects. *BMC Genomics* **20**, 223 (2019).

21. Prevosti, A., Ribo, G., Serra, L., Aguade, M., Balaña, J., Monclus, M. & Mestres, F. Colonization of America by *Drosophila subobscura*: Experiment in natural populations that supports the adaptive role of chromosomal-inversion polymorphism *Proc. Natl. Acad. Sci. U.S.A.* **85**, 5597–5600 (1988).

22. Rodríguez-Trelles, F., Alvarez, G. & Zapata, C. Time-series analysis of seasonal changes of the O inversion polymorphism of *Drosophila subobscura*. *Genetics* **142**, 179–187 (1996).

23. Rodríguez-Trelles, F., Tarrío, R. & Santos, M. Genome-wide evolutionary response to a heat wave in *Drosophila*. *Biol. Lett.* **9**, 20130228 (2013).

24. Balanyà, J., Solé, E., Oller, J. M., Sperlich, D. & Serra, L. Long-term changes in the chromosomal inversion polymorphism of *Drosophila subobscura*: II. European populations. *J. Zool. Syst. Evol. Res.* **42**, 191–201 (2004).

25. Shorthouse, D. P. SimpleMappr, an online tool to produce publication-quality point maps. (2010) (Retrieved from https://www.simplemappr.net accessed January 31, 2024).

26. Pausas, J. G. & Millán, M. M. Greening and browning in a climate change hotspot: the Mediterranean Basin. *BioScience*, **69**, 143–151 (2019).

27. Rodríguez-Trelles, F. & Tarrío, R. Data and code for 'Acceleration of *Drosophila subobscura* evolutionary response to global warming in Europe'. figshare https://doi.org/10.6084/m9.figshare.24619629 (2024).

28. Russo, S., Sillmann, J. & Fischer, E. M. Top ten European heatwaves since 1950 and their occurrence in the coming decades. *Environ. Res. Lett.* **10**, 124003 (2015).

29. Zhang, R., Sun, C., Zhu, J., Zhang, R. & Li, W. Increased European heat waves in recent decades in response to shrinking Arctic sea ice and Eurasian snow cover. *NPJ Clim. Atmos. Sci.* **3**, 7 (2020).

30. Lhotka, O. & Kyselý, J. The 2021 European heat wave in the context of past major heat waves. *Earth Space Sci*. **9**, e2022EA002567 (2022).

31. Grant, P. R., Grant, B. R., Huey, R. B., Johnson, M. T. J., Knoll, A. H. & Schmitt, J. Evolution caused by extreme events. *Philos*. *Trans*. *R*. *Soc*. *Lond*. *B Biol*. *Sci*. **372**, 20160146 (2017).

32. Ma, C. S., Ma, G. & Pincebourde, S. Survive a warming climate: Insect responses to extreme high temperatures. *Annu*. *Rev*. *Entomol*. **66**, 163–184 (2021).

33. Jørgensen, L. B., Ørsted, M., Malte, H., Wang, T. & Overgaard, J. Extreme escalation of heat failure rates in ectotherms with global warming. *Nature* **611**, 93–98 (2022).

34. Meehl, G. A. & Tebaldi, C. More intense, more frequent, and longer lasting heat waves in the 21st century. *Science* **305**, 994–997 (2004).

35. Rego, C., Balanyà, J., Fragata, I., Matos, M., Rezende, E. L. & Santos, M. Clinal patterns of chromosomal inversion polymorphisms in *Drosophila subobscura* are partly associated with thermal preferences and heat stress resistance. *Evolution* **64**, 385–97 (2010).

36. Kingsolver, J. G., Woods, H. A., Buckley, L. B., Potter, K. A., MacLean, H. J. & Higgins, J. K. Complex life cycles and the responses of insects to climate change. *Integr Comp Biol.* **51**, 719–32 (2011).

37. Barrett, R. D. & Schluter, D. Adaptation from standing genetic variation. *Trends Ecol*. *Evol*. **23**, 38–44 (2008).

38. Bitter, M. C., Kapsenberg, L., Gattuso, J. P. & Pfister, C. A. Standing genetic variation fuels rapid adaptation to ocean acidification. *Nat*. *Commun*. **10**, 5821 (2019).

39. Matuszewski, S., Hermisson, J. & Kopp, M. Catch me if you can: Adaptation from standing genetic variation to a moving phenotypic optimum. *Genetics* **200**, 1255–1274 (2015).

40. Radchuk, V., Reed, T., Teplitsky, C., van de Pol, M., Charmantier, A., Hassall, C., Adamík, P., Adriaensen, F., Ahola, M. P., Arcese, P., Miguel Avilés, J., Balbontin, J., Berg, K. S., Borras, A., Burthe, S., Clobert, J., Dehnhard, N., de Lope, F., Dhondt, A. A., Dingemanse, N. J., Doi, H., Eeva, T., Fickel, J., Filella, I., Fossøy, F., Goodenough, A. E., Hall, S. J. G., Hansson, B., Harris, M., Hasselquist, D., Hickler, T., Joshi, J., Kharouba, H., Martínez, J. G., Mihoub, J. B., Mills, J. A., Molina-Morales, M., Moksnes, A., Ozgul, A., Parejo, D., Pilard, P., Poisbleau, M., Rousset, F., Rödel, M. O., Scott, D., Senar, J. C., Stefanescu, C., Stokke, B. G., Kusano, T., Tarka, M., Tarwater, C. E., Thonicke, K., Thorley, J., Wilting, A., Tryjanowski, P., Merilä, J., Sheldon, B. C., Pape Møller, A., Matthysen, E., Janzen, F., Dobson, F. S., Visser, M. E., Beissinger, S. R., Courtiol, A. & Kramer-Schadt, S. Adaptive responses of animals to climate change are most likely insufficient. *Nat Commun*. **10**, 3109 (2019).

41. Harvey, J. A., Thakur, M. P. & Ellers, J. The tarnished silver lining of extreme climatic events. *Trends Ecol*. *Evol*. **36**, 384–385 (2021).

42. Parmesan, C. & Singer, M. C. Mosaics of climatic stress across species' ranges: tradeoffs cause adaptive evolution to limits of climatic tolerance. *Philos*. *Trans*. *R*. *Soc*. *Lond*. *B Biol*. *Sci*. **377**, 20210003 (2022).

43. Abarca, M. & Spahn, R. Direct and indirect effects of altered temperature regimes and phenological mismatches on insect populations. *Curr*. *Opin*. *Insect*. *Sci*. **47**, 67–74 (2021).

44. Harvey, J. A., Tougeron, K., Gols, R., Heinen, R., Abarca, M., Abram, P. K., Basset, Y., Berg, M., Boggs, C., Brodeur, J., Cardoso, P., de Boer, J. G., De Snoo, G. R., Deacon, C., Dell, J. E., Desneux, N., Dillon, M. E., Duffy, G. A., Dyer, L., Ellers, J., Espíndola, A., Fordyce, J., Forister, M. L., Fukushima, C., Gage, M. J. G., García-Robledo, C., Gely, C., Gobbi, M., Hallmann, C., Hance, T., Harte, J., Hochkirch, A., Hof, C., Hoffmann, A. A., Kingsolver, J. G. Lamarre, G. P. A., Laurance, W. F., Lavandero, B., Leather, S. R., Lehmann, P., Le Lann, C., López-Uribe, M. M., Ma, C.-S., Ma, G., Moiroux, J., Monticelli, L., Nice, C., Ode, P. J., Pincebourde, S., Ripple, W. J., Rowe, M., Samways, M. J., Sentis, A., Shah, A. A., Stork, N., Terblanche, J. S., Thakur, M. P., Thomas, M. B., Tylianakis, J. M., Van Baaren, J., Van de Pol, M., Van der Putten, W. H., Van Dyck, H., Verberk, W. C. E. P., Wagner, D. L., Weisser, W. W., Wetzel, W. C., Woods, H. A., Wyckhuys, K. A. G. & Chown, S. L. Scientists' warning on climate change and insects. *Ecol*. *Monogr*. **93**, e1553 (2023).

45. Des Roches, S., Post, D. M., Turley, N. E., Bailey, J. K., Hendry, A. P., Kinnison, M. T., Schweitzer, J. A. & Palkovacs, E. P. The ecological importance of intraspecific variation. *Nat*. *Ecol*. *Evol*. **2**, 57–64 (2018).

46. Diamond, S. E. & Martin, R. A. Evolution is a double-edged sword, not a silver bullet, to confront global change. *Ann*. *N.Y*. *Acad*. *Sci*. **1469**, 38–51 (2020).

47. Roesti, M., Gilbert, K. J. & Samuk, K. Chromosomal inversions can limit adaptation to new environments. *Mol*. *Ecol*. **31**, 4435–4439 (2022).

48. Gossner, M. M., Menzel, F. & Simons, N. K. Less overall, but more of the same: drivers of insect population trends lead to community homogenization. *Biol*. *Lett*. **19**, 20230007 (2023).

49. Nunez, J. C. B., Lenhart, B. A., Bangerter, A., Murray, C. S., Mazzeo, G. R., Yu, Y., Nystrom, T. L., Tern, C., Erickson, P. A. & Bergland, A. O. A cosmopolitan inversion facilitates seasonal adaptation in overwintering *Drosophila*. *Genetics* **226**, iyad207 (2024).

50. Berdan, E. L., Barton, N. H., Butlin, R., Charlesworth, B., Faria, R., Fragata, I., Gilbert, K. J., Jay, P., Kapun, M., Lotterhos, K. E., Mérot, C., Durmaz Mitchell. E., Pascual. M., Peichel, C. L., Rafajlović, M., Westram, A. M., Schaeffer, S. W., Johannesson, K. & Flatt, T. How chromosomal inversions reorient the evolutionary process. *J. Evol. Biol.* **36**, 1761–1782 (2023).

51. Karageorgiou, C., Tarrío, R. & Rodríguez-Trelles, F. The cyclically seasonal *Drosophila subobscura* inversion O_7 originated from fragile genomic sites and relocated immunity and metabolic genes. *Front. Genet.* **11**, 565836 (2020).

52. González-Tokman, D., Córdoba-Aguilar, A., Dáttilo, W., Lira-Noriega, A., Sánchez-Guillén, R. A. & Villalobos, F. Insect responses to heat: physiological mechanisms, evolution and ecological implications in a warming world. *Biol*. *Rev*. **95**, 802–821 (2020).

53. Smith, S., Edmonds, J., Hartin, C., Mundra, A. & Calvin, K. Near-term acceleration in the rate of temperature change. *Nature Clim*. *Change*. **5**, 333–336 (2015).

54. Li, C., Fang, Y., Caldeira, K., Zhang, X., Diffenbaugh, N. S. & Michalak, A. M. Widespread persistent changes to temperature extremes occurred earlier than predicted. *Sci*. *Rep*. **8**, 1007 (2018).

55. Diffenbaugh, N. S. & Barnes, E. A. Data-driven predictions of the time remaining until critical global warming thresholds are reached. *Proc. Natl. Acad. Sci. U.S.A.* **120**, e2207183120 (2023).

56. Willcock, S., Cooper, G. S., Addy, J. & Dearing, J. A. Earlier collapse of Anthropocene ecosystems driven by multiple faster and noisier drivers. *Nat. Sustain.* **6**, 1331–1342 (2023).

57. Rodríguez-Trelles, F. & Rodríguez, M. Á. Comment on "Global genetic change tracks global climate warming in *Drosophila subobscura*. *Science* **315**, 1497 (2007).

58. Solé, E. "Análisi dels cambis cromosòmics a llarg termini en poblacions naturals de *Drosophila subobscura* i la seva relació amb el possible canvi climàtic global." PhD Thesis, University of Barcelona https://www.tesisenred.net/handle/10803/1849#page=1 (2002).

59. Crawley, M. J. *The R Book* (John Wiley & Sons Ltd., 2013).

60. Buckley, L. B. & Huey, R. B. Temperature extremes: geographic patterns, recent changes, and implications for organismal vulnerabilities. *Glob. Change Biol.* **22**, 3829–3842 (2016).

61. R Development Core Team. R: a language and environment for statistical computing (2020).

62. Mazerolle, M. J. AICcmodavg: Model selection and multimodel inference based on (Q)AIC(c). R package version 2.3-1 (2020).

63. Bivand, R. "R packages for analyzing spatial sata: A comparative case study with areal data." *Geogr. Anal.* **54**, 488–518 (2022).

Methods

Sampling approach

All methods were as in ref.[14]. Flies were collected between 2015 and 2019 at the same 12 continental European locations (Groningen [the Netherlands], Louvain-la-Neuve [Belgium], Tübingen [Germany], Vienna [Austria], Leuk [Switzerland], Lagrasse, Montpellier, and Villars [France], and Málaga, Punta Umbría, Riba-roja de Túria, and Queralbs [Spain]) (Fig. 1) and nearly the same dates of the year previously used in ref.[14]. To avoid bias arising from neglect of the regular seasonal cycles of inversions in the sampling approach[57], the average absolute difference in number of days between the sampling dates of R2 and R1 was kept as small as possible (15.2 ± 14.7 days), given the occasional occurrence of unfavorable sampling weather conditions. Additionally, a sign test of the direction of the differences was non-significant (p = 0.774, n = 12). Geographical coordinates and date information were obtained from refs.[14,58] (Supplementary Table 1[27]).

Polytene chromosome preparation and inversion scoring

For each sample, chromosome arrangement frequencies were scored following standard methods (*e.g.*, ref.[14]). First, wild-caught males or F1 males from wild-caught females were individually crossed with virgin females of the *ch-cu* strain, which is structurally homozygous for the A_{ST}, J_{ST}, U_{ST}, E_{ST}, and O_{3+4} chromosome arrangements. The polytene chromosomes of one F1 female third-instar larva from each cross were then analyzed to determine the configuration of one haploid chromosome set from the wild (Supplementary Table 1[27]).

The chromosomal polymorphisms in this current second resurvey (R2) were compared with those from the same locations collected 18.4 ± 2.2 years earlier in the first resurvey (R1) and 49.2 ± 7.3 years earlier in the historical survey (HS)[14].

Mean temperature data and chromosome arrangement frequency analyses

Balanyá et al. (2006)[14] used standard Principal Components Analysis (PCA) to combine climatic variables and chromosome arrangement frequencies into single indices (first principal components, denoted as T_{PC1} and Ch_{PC1}, respectively). T_{PC1} was shown to represent the latitudinal gradient in mean temperature across sites, with high-positive (negative) values corresponding to a warmer (cooler) site. Analogously, Ch_{PC1} was shown to represent the latitudinal gradient in chromosome arrangement composition across sites, with high-positive (negative) values corresponding to a polymorphism associated with warmer (cooler) sites.

Following ref.[14], we built a 36 rows (12 sites times three surveys) by 48 columns matrix of monthly mean temperature data for the four years immediately prior to each sample from the nearest weather station for each population gathered using NASA GISS (http://data.giss.nasa.gov/gistemp/station_data_v4/). Likewise, we built a 36 by 45 matrix of $2\sqrt{p_{ij}}$ transformed inversion frequency records, i being the ith population and j the jth arrangement. We then conducted centered unscaled PCAs on these two matrices to obtain the respective first principal component-based climate (T_{PC1}) and genomewide chromosome (Ch_{PC1}) indices. T_{PC1} and Ch_{PC1} accounted for 85.2% and 68.9% of the original variances, respectively.

T_{PC1} values are highly collinear with those obtained using the explicit mean temperature data (T) directly (two-tailed Pearson's r T_{PC1} vs T = 1.000, 1.000, and 0.999 respectively for HS, R1 and R2, $p < 10^{-5}$ and n =12 in the three cases). Likewise, Ch_{PC1} values are highly collinear with those obtained using the genome-wide warm dose (WD), an alternative genome-wide index defined as

the average across the five-chromosome set of one minus the frequency of the Standard cold-climate arrangement[23] (two-tailed Pearson's r Ch_{PC1} vs WD = 0.974, 0.994, and 0.969 respectively for HS, R1 and R2, $p < 1 \times 10^{-5}$ and $n = 12$ in the three cases).

The relationships between variables were characterized considering three types of models, comprising simple linear, two-segment piecewise linear, and second-order polynomial models (Supplementary Tables 2, 4, 6, and 7). Best-fit model selection was done using one-way ANOVA for nested comparisons between linear and piecewise or second-order polynomial models, and Akaike's information criterion with small sample correction for non-nested comparisons between piecewise and second-order polynomial models (Supplementary Tables 2, 3, and 8).

Visual inspection of the scatterplot of T_{PC1} against latitude (Fig. 2, a and b) suggested a threshold response, with distinct patterns of the response variable above and below the center of the latitudinal range in both cases. We ran two-segment piecewise regression analyses[59], targeted to the three centralmost latitudes (from 43.8º to 46.3º, which equates to a stretch of ~278km, assuming ~111km per degree of latitude) and keeping the results from each coordinate. A piecewise model with a break at 46.3º provides a significant improvement over the unsegmented linear model (Supplementary Table 2) and the second-order polynomial model (Supplementary Table 3) in all the three surveys. This value should not be taken as an absolute location, but as a transition zone between the Mediterranean and temperate climatic regions of western Europe (Fig. 1). As expected if the chromosomal inversion polymorphisms respond to the thermal environment, piecewise regression also detects a break at 46.3º for Ch_{PC1} in the three surveys (Supplementary Table 2). In this case, however, the transition zone extends to 45.4º and 43.8º, and the variation can be similarly well described using a second-order polynomial model (Supplementary Table 3). The observed greater broadness of the genetic threshold compared to the temperature threshold is likely an indication of potentially maladaptive homogenizing gene flow. With respect to the relationship of Ch_{PC1} with T_{PC1}, second-order polynomial models and piecewise models outperform the linear baselines (Supplementary Table 2), and the two models are globally similar when compared to one another (Supplementary Table 3).

Decadal rates of change (Fig. 3) were calculated for T_{PC1} and Ch_{PC1}, and individually for each of the five A, J, U, E, and O chromosomes using one minus the frequency of the corresponding Standard cold-climate arrangement[23].

Heat wave and extreme temperature data analyses.

We developed a crude index of a site exposure to heat waves (*HWe*) based on the results by ref.[30]. The study provides a description of all major heat waves that hit Europe since 1950. For each heat wave, the event was assigned within one or more of nine predefined regions of 5º latitude by 5º longitude, and a map of accumulated temperature anomaly was produced using a discrete color scale. Our survey sites are distributed in three of the nine regions: south Europe (ML, PU, and RT), south-western Europe (QR, LG, and MP), and central Europe (VL, LK, VN, TB, LN, and GR). *HWe* was determined for each sample site separately as follows: first, for each individual heat wave, sites outside the assigment regions were given a score of zero, while sites inside the regions were given a score 0 to 6, depending on the magnitude of the anomaly. Next, for each site the sum of the scores for all events was divided by the number of decades elapsed separately for the HS-R1 and R1-R2 periods.

The relationship between the Ch_{PC1} index and extreme temperature was evaluated using the monthly maximum (*TXx*) and monthly minimum (*TNn*) of daily temperatures. The two metrics

have been considered to be appropriate for examining effects of environmental thermal stress on small-sized ectotherms such as *D. subobscura*[60]. We employed the same methodological approach as that used in the mean temperature analysis. Corresponding 36 by 48 matrices were built using *TXx* and *TNn* data collected using ECA&D (https://www.ecad.eu/download/millennium/millennium.php) and subjected to PCA analysis to derive PC1-based *TXx* (TXx_{PC1}) and *TNn* (TNn_{PC1}) indices. TXx_{PC1} and TNn_{PC1} accounted for 65.8% and 78.3% of the original variances, respectively. The values of the two indices are highly similar to those obtained using the explicit *TXx* and *TNn* data directly (two-tailed Pearson's *r* TXx_{PC1} vs *TXx* = 0.998, 0.998, and 0.997, and two-tailed Pearson's *r* TNn_{PC1} vs *TNn* = 1.000, 1.000, and 1.000, respectively for HS, R1 and R2, $p < 10^{-5}$ and $n = 12$ in all six cases). The change of Ch_{PC1} with TXx_{PC1} and with TNn_{PC1} was described using second-order polynomial regression (Supplementary Table 7).

We used Microsoft Excel for data preparation. All statistical analyses were performed using R version 4.2.1 (R Core Team, 2020)[61]. Principal component analyses (PCA) (Fig. 2 A, B and C), Spearman's rho correlation analyses (Table 1), regression analyses including linear, piecewise and nonlinear second-order polynomial regression analyses (Fig. 2 A, B and C; Supplementary Tables 2, 4 and 6), and Wilcoxon signed rank and Mann-Withney U tests (Supplementary Table 5) were performed using the 'prcomp', 'cor.test', 'lm' and 'wilcox.test' functions built into the base R environment[61], respectively. Akaike's Information Criteria (AIC) model selection analyses (Supplementary Tables 3 and 8) were performed using the 'aictab' function in the 'AICcmodvag' package[62]. Moran's I tests of spatial autocorrelation were performed using the 'moran.i' function in the 'spedep' package[63]. Boxplot graphs (Fig. 3) were created using the 'boxplot' and 'stripchart' functions in base R[61].

Data availability

All data generated in this study are available in the main text and the supplementary information, and can also be accessed on Figshare at https://doi.org/10.6084/m9.figshare.24619629 (ref.[27])

Code availability

The R code for our statistical analyses can be accessed on Figshare at https://doi.org/10.6084/m9.figshare.24619629 (ref.[27])

Methods-only references

57. Rodríguez-Trelles, F. & Rodríguez, M. Á. Comment on "Global genetic change tracks global climate warming in *Drosophila subobscura*. *Science* **315**, 1497 (2007).
58. Solé, E. "Análisi dels cambis cromosòmics a llarg termini en poblacions naturals de *Drosophila subobscura* i la seva relació amb el possible canvi climàtic global." PhD Thesis, University of Barcelona [https://www.tesisenred.net/handle/10803/1849#page=1] (2002).
59. Crawley, M. J. *The R Book* (John Wiley & Sons Ltd., 2013).

60. Buckley, L. B. & Huey, R. B. Temperature extremes: geographic patterns, recent changes, and implications for organismal vulnerabilities. *Glob. Change Biol.* **22**, 3829–3842 (2016).

61. R Development Core Team. R: a language and environment for statistical computing (2020).

62. Mazerolle, M. J. AICcmodavg: Model selection and multimodel inference based on (Q)AIC(c). R package version 2.3-1 (2020).

63. Bivand, R. "R packages for analyzing spatial sata: A comparative case study with areal data." *Geogr. Anal.* **54**, 488–518 (2022).

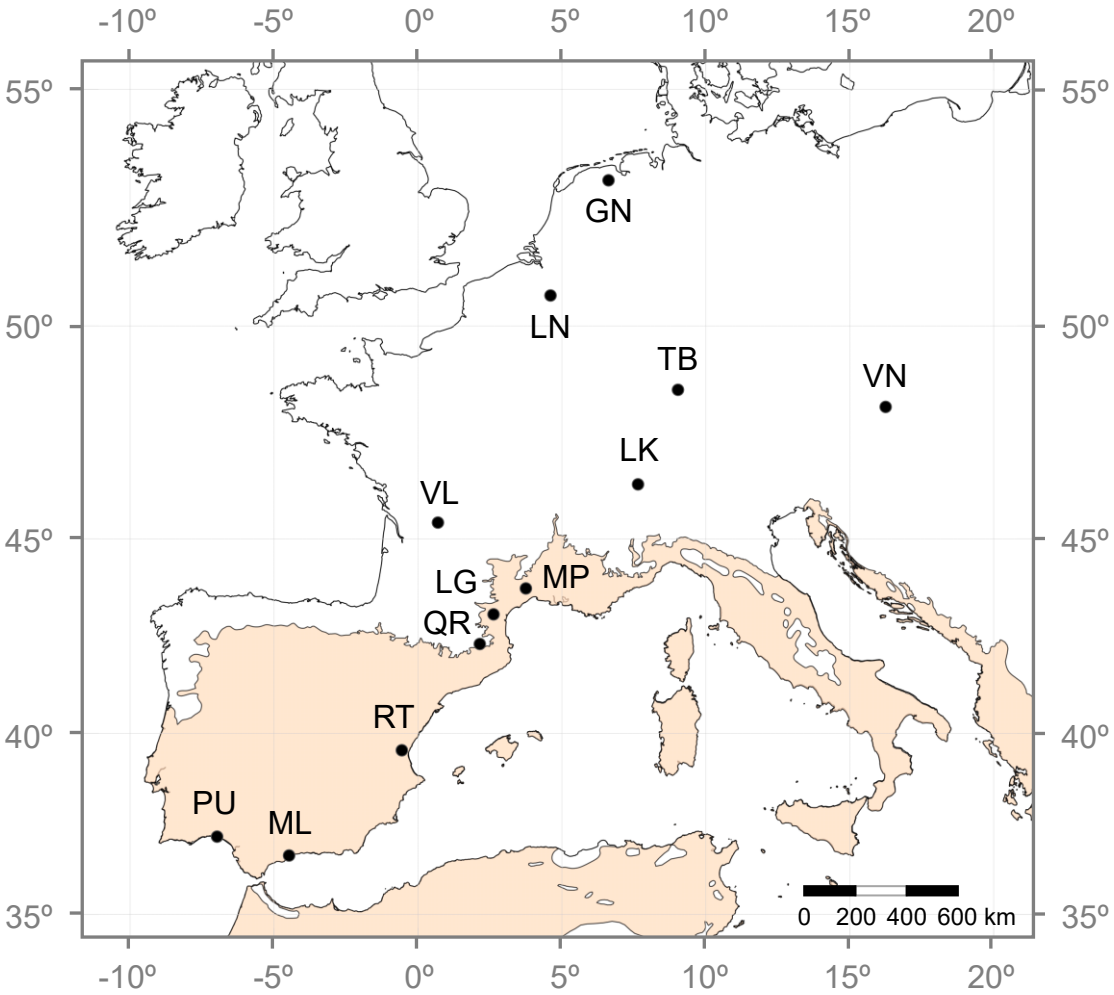

Mediterranean

Temperate

ML	Málaga	VL	Villars
PU	Punta Umbría	LK	Leuk
RT	Riba-roja de Túria	VN	Vienna
QR	Queralbs	TB	Tübingen
LG	Lagrasse	LN	Louvain-la-Neuve
MP	Montpellier	GN	Groningen

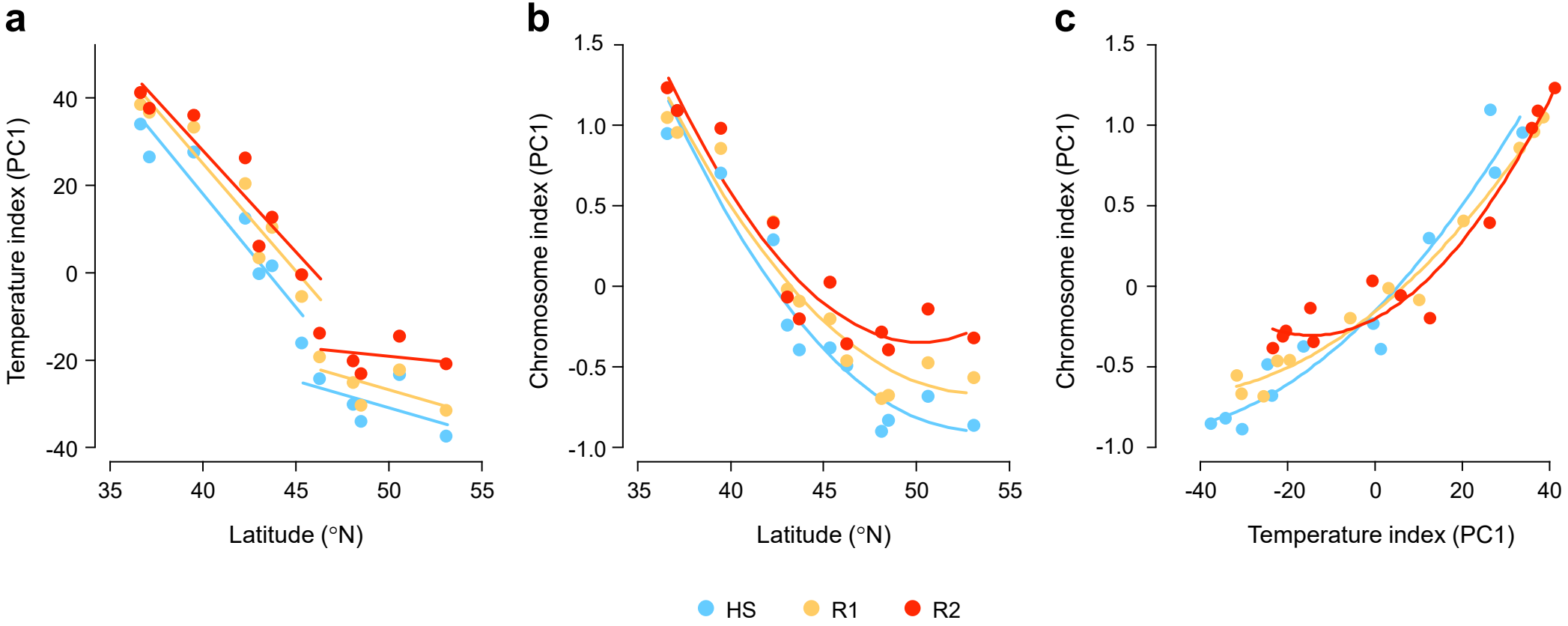
a
b
c
Temperature index (PC1)
Chromosome index (PC1)
Chromosome index (PC1)
Latitude (°N)
Latitude (°N)
Temperature index (PC1)
40
20
0
-20
-40
1.5
1.0
0.5
0
-0.5
-1.0
35
40
45
50
55
-40
-20
0
20
40
HS
R1
R2

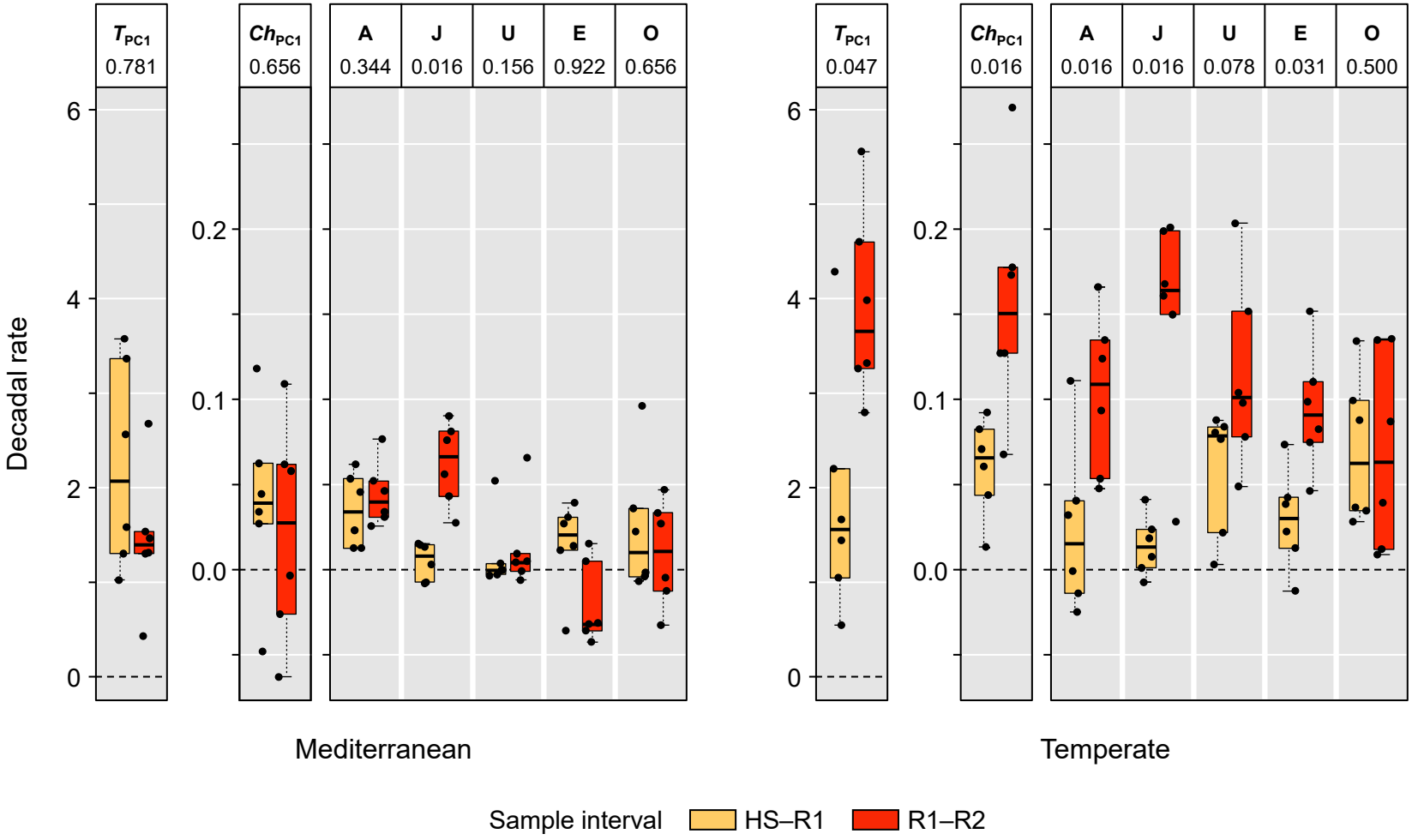
T_{PC1}
0.781
Ch_{PC1}
0.656
A
0.344
J
0.016
U
0.156
E
0.922
O
0.656
T_{PC1}
0.047
Ch_{PC1}
0.016
A
0.016
J
0.016
U
0.078
E
0.031
O
0.500
Decadal rate
0
2
4
6
0.0
0.1
0.2
Mediterranean
Temperate
Sample interval
HS–R1
R1–R2

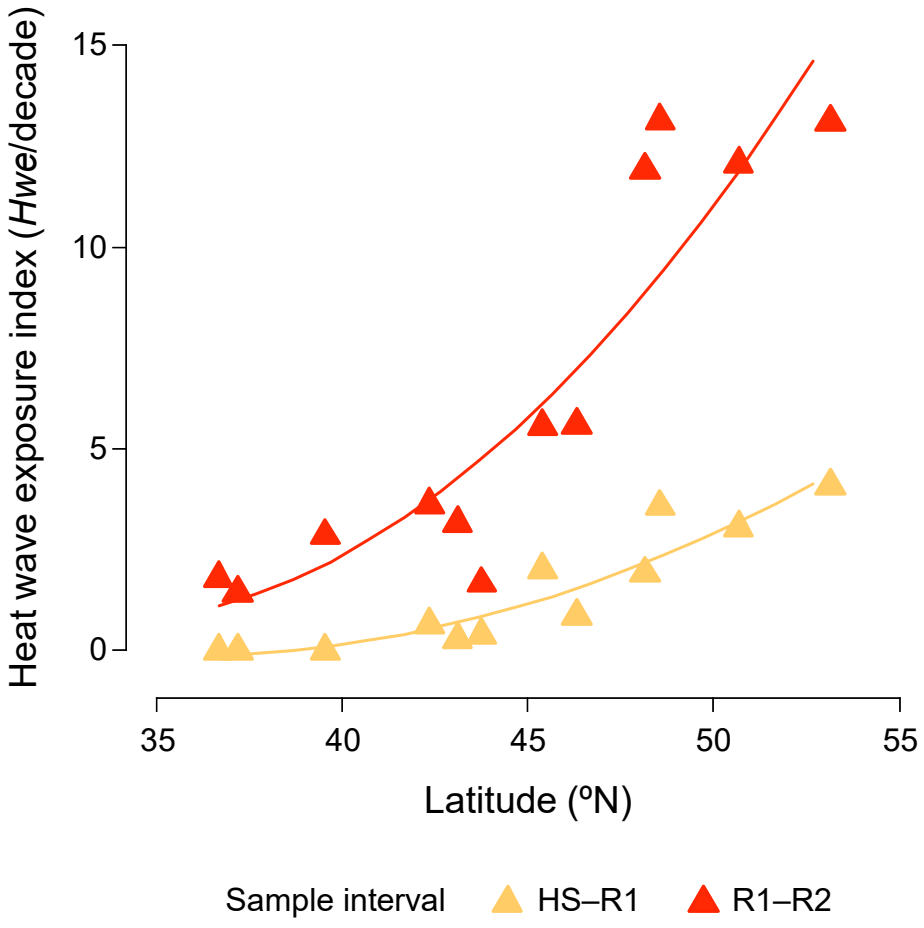
Heat wave exposure index (Hwe/decade)
15
10
5
0
35
40
45
50
55
Latitude (ºN)
Sample interval
HS–R1
R1–R2

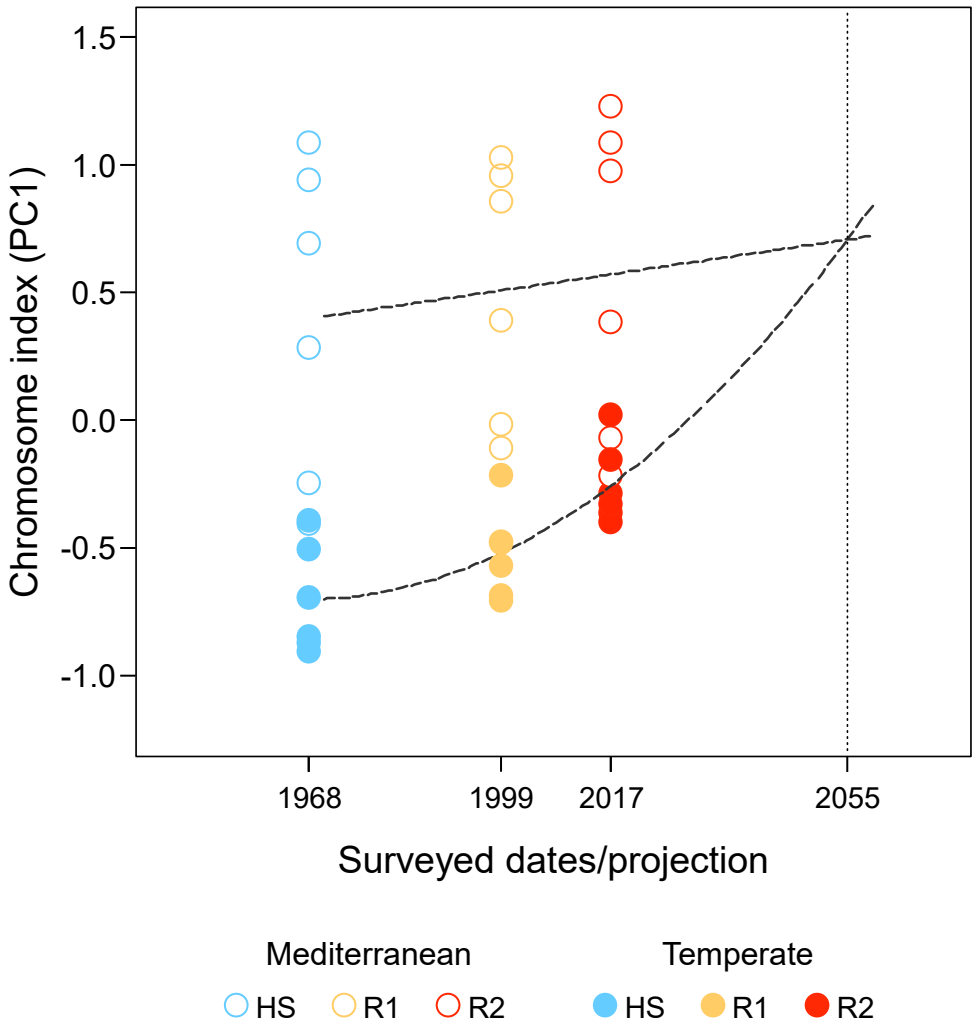
1.5
1.0
0.5
0.0
-0.5
-1.0
Chromosome index (PC1)
1968
1999
2017
2055
Surveyed dates/projection
Mediterranean
HS
R1
R2
Temperate
HS
R1
R2

Table of Contents

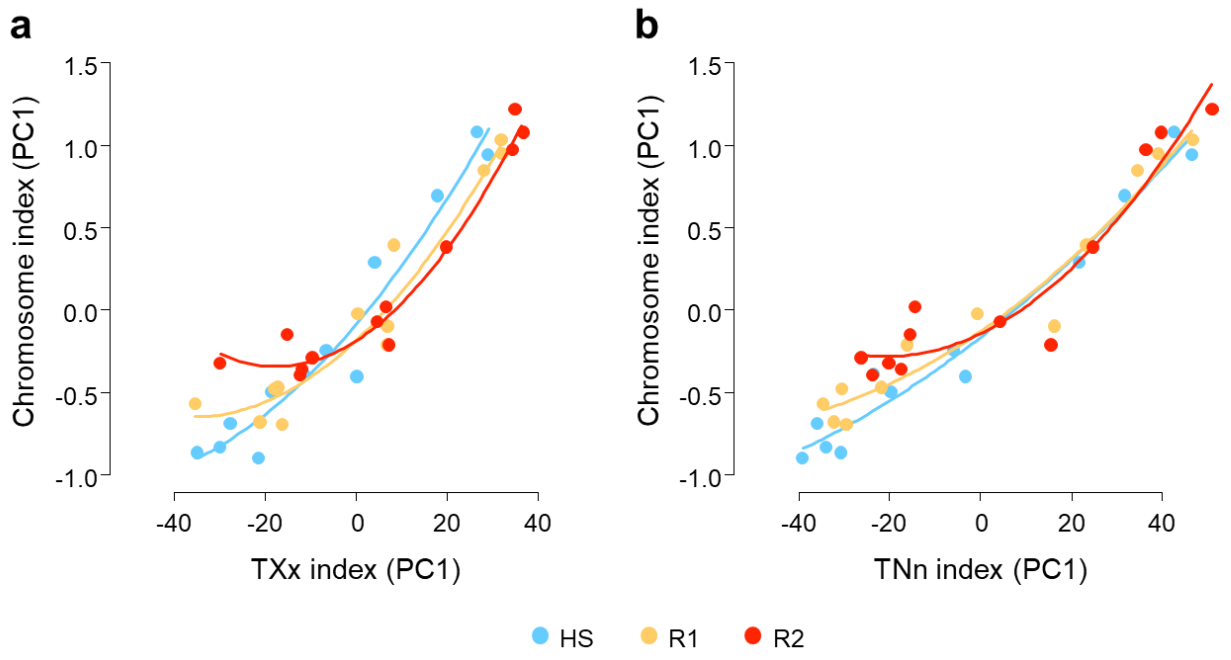

Supplementary Figure 1 | Second-order polynomial relationship between the chromosome index (Ch_{PC1}) and the (a) extreme maximum temperature (TXx_{PC1}) and (b) extreme minimum temperature (TNn_{PC1}) indices (Supplementary Table 8).

Supplementary Table 1 | Geographical coordinates, collection dates, chromosome arrangement frequencies, and sample sizes (N) for the updated historical records of chromosomal inversion polymorphisms at 12 European *D. subobscura* locations (ref.[27]; also accessible from figshare at https://doi.org/10.6084/m9.figshare.24619629)

	Málaga	**Punta Umbría**	**Riba-roja de Túria**	**Queralbs**	**Lagrasse**	**Montpellier**	**Villars**	**Leuk**	**Vienna**	**Tübingen**	**Louvain-la-Neuve**	**Groningen**
Coordinates WGS84	36.66635, - 4.47747	37.18557, -6.97836	39.55035, -0.55921	42.34604, 2.14905	43.10536, 2.62638	43.76044, 3.74990	45.39132, 0.69424	46.32103, 7.64518	48.15108, 16.24883	48.54652, 9.03370	50.67341, 4.60543	53.14481, 6.62071
Collection date	April 2, 2015	May 11, 2019	March 22, 2019	June 22, 2019	October 21, 2016	October 19, 2016	September 8, 2019	August 27, 2016	August 20, 2016	August 24, 2016	August 26-27, 2018	August 22-24, 2018
A_{ST}	0.110	0.184	0.182	0.299	0.473	0.514	0.558	0.368	0.352	0.517	0.457	0.505
A_1	0.000	0.000	0.050	0.037	0.241	0.308	0.239	0.402	0.486	0.325	0.219	0.330
A_2	0.890	0.806	0.769	0.664	0.286	0.178	0.204	0.230	0.162	0.158	0.324	0.165
A_{2+6}	0.000	0.010	0.000	0.000	0.000	0.000	0.000	0.000	0.000	0.000	0.000	0.000
N	127	103	121	107	112	107	113	87	105	120	105	103
J_{ST}	0.094	0.126	0.132	0.112	0.357	0.299	0.186	0.368	0.228	0.317	0.234	0.272
J_1	0.906	0.874	0.868	0.888	0.643	0.701	0.814	0.632	0.772	0.683	0.766	0.728
N	127	103	121	107	112	107	113	106	114	120	107	103
U_{ST}	0.000	0.010	0.008	0.037	0.045	0.140	0.080	0.208	0.219	0.225	0.131	0.262
U_1	0.000	0.000	0.000	0.000	0.000	0.000	0.000	0.028	0.035	0.025	0.000	0.000
U_2	0.000	0.000	0.000	0.000	0.000	0.000	0.000	0.000	0.000	0.000	0.009	0.000
U_{1+2}	0.472	0.466	0.463	0.757	0.848	0.766	0.726	0.717	0.649	0.675	0.748	0.650
U_{1+2+6}	0.000	0.000	0.000	0.000	0.009	0.009	0.000	0.009	0.009	0.008	0.000	0.000
U_{1+2+8}	0.528	0.524	0.529	0.206	0.098	0.084	0.195	0.038	0.088	0.067	0.112	0.087
N	127	103	121	107	112	107	113	106	114	120	107	103
E_{ST}	0.197	0.262	0.256	0.542	0.589	0.682	0.487	0.651	0.544	0.717	0.598	0.641
E_8	0.000	0.039	0.025	0.037	0.027	0.037	0.009	0.057	0.132	0.050	0.019	0.019
E_{1+2}	0.197	0.272	0.174	0.196	0.250	0.159	0.327	0.179	0.070	0.158	0.308	0.252
E_{1+2+9}	0.205	0.078	0.124	0.093	0.098	0.093	0.027	0.094	0.228	0.067	0.019	0.029
$E_{1+2+9+3}$	0.024	0.068	0.041	0.019	0.009	0.009	0.035	0.000	0.000	0.000	0.000	0.010
$E_{1+2+9+12}$	0.378	0.282	0.380	0.112	0.027	0.019	0.115	0.019	0.026	0.008	0.056	0.049
N	127	103	121	107	112	107	113	106	114	120	107	103
O_{ST}	0.024	0.010	0.050	0.318	0.339	0.421	0.319	0.377	0.421	0.467	0.374	0.485
O_5	0.000	0.000	0.000	0.000	0.000	0.000	0.000	0.009	0.000	0.000	0.000	0.000
O_6	0.000	0.000	0.000	0.000	0.000	0.009	0.000	0.009	0.009	0.000	0.009	0.000
O_7	0.008	0.000	0.008	0.009	0.000	0.000	0.000	0.000	0.000	0.000	0.000	0.000
O_{3+4}	0.252	0.320	0.355	0.262	0.277	0.224	0.292	0.226	0.307	0.250	0.187	0.165
O_{3+4+1}	0.000	0.000	0.000	0.000	0.000	0.000	0.000	0.000	0.026	0.017	0.000	0.000
O_{3+4+2}	0.031	0.000	0.000	0.028	0.027	0.009	0.000	0.000	0.018	0.017	0.009	0.049
O_{3+4+7}	0.622	0.485	0.413	0.056	0.009	0.028	0.009	0.000	0.000	0.000	0.000	0.000
O_{3+4+8}	0.047	0.126	0.124	0.290	0.339	0.252	0.363	0.340	0.132	0.233	0.411	0.301
O_{3+4+18}	0.000	0.000	0.000	0.000	0.000	0.000	0.000	0.000	0.009	0.000	0.000	0.000
O_{3+4+22}	0.016	0.039	0.050	0.037	0.009	0.028	0.009	0.028	0.070	0.017	0.000	0.000
$O_{3+4+16+2}$	0.000	0.019	0.000	0.000	0.000	0.028	0.009	0.009	0.009	0.000	0.009	0.000
N	127	103	121	107	112	107	113	106	114	120	107	103

Supplementary Table 2 | One-way ANOVA F tests for the fit of second-order polynomial models and two-segment linear piecewise regression models to the relationships of T_{PC1} and Ch_{Pc1} with latitude and of Ch_{PC1} with T_{PC1}, in comparison to simple linear models. In the case of the relationship of T_{PC1} vs latitude, only the piecewise model outperforms the linear model, consistently indicating a break at 46.3º in all three surveys. In the cases of Ch_{PC1} vs latitude and Ch_{PC1} vs T_{PC1}, both models showed an overall significantly better performance than the linear model, and the piecewise model indicates an extended boundary across the three breaks.

		Second-order polynomial model			Two-segment piecewise linear model with break at latitude:								
					43.8º			45.4º			46.3º		
T_{PC1} vs Latitude	Survey	Adj. r^2	$F_{[9,1]}$	P	Adj. r^2	$F_{[8,2]}$	P	Adj.r^2	$F_{[8,2]}$	P	Adj. r^2	$F_{[8,2]}$	P
	HS	0.906	1.860	0.206	0.909	1.600	0.261	0.950	6.126	0.024	0.945	5.156	0.036
	R1	0.907	1.355	0.274	0.900	0.746	0.504	0.941	3.973	0.063	0.959	7.429	0.015
	R2	0.882	1.882	0.203	0.874	1.080	0.385	0.918	3.801	0.069	0.944	7.511	0.015
		Second-order polynomial model			Two-segment piecewise linear model with break at latitude:								
					43.8º			45.4º			46.3º		
Ch_{PC1} vs Latitude	Survey	Adj. r^2	$F_{[9,1]}$	P	Adj. r^2	$F_{[8,2]}$	P	Adj. r^2	$F_{[8,2]}$	P	Adj. r^2	$F_{[8,2]}$	P
	HS	0.937	12.625	0.006	0.943	8.025	0.012	0.934	6.320	0.023	0.938	6.959	0.018
	R1	0.924	10.797	0.009	0.923	5.758	0.028	0.932	6.991	0.018	0.955	12.822	0.003
	R2	0.900	17.337	0.002	0.923	12.539	0.003	0.913	10.737	0.005	0.906	9.575	0.008
		Second-order polynomial model			Two-segment piecewise linear model with break at T_{PC1}:								
					-16.48			-0.61			1.28		
Ch_{PC1} vs T_{PC1}	Survey	Adj. r^2	$F_{[9,1]}$	P	Adj. r^2	$F_{[8,2]}$	P	Adj.r^2	$F_{[8,2]}$	P	Adj. r^2	$F_{[8,2]}$	P
	HS	0.935	4.483	0.063	0.913	1.063	0.390	0.945	4.461	0.050	0.947	4.366	0.052
					-5.81			2.99			10.01		
	R1	0.981	17.319	0.002	0.968	3.739	0.071	0.977	6.536	0.021	0.989	18.682	0.001
					-0.77			5.79			12.38		
	R2	0.942	18.912	0.002	0.888	3.188	0.096	0.949	11.807	0.004	0.982	41.721	0.000

Supplementary Table 3 | Akaike Information Criterion with small-sample correction (AICc) and Akaike weights (AICc-Wt) for the relative fit of second-order polynomial and two-segment piecewise regression models to the relationships of T_{PC1} and Ch_{Pc1} with latitude, and of Ch_{PC1} with T_{PC1}. In the case of the relationship T_{PC1} vs latitude, the piecewise model with a break at 46.3º produces lower AICc scores than the second-order polynomial model in all three surveys. In the cases of Ch_{PC1} vs latitude and Ch_{PC1} vs T_{PC1}, neither a specific piecewise model nor the second-order polynomial model consistently outperforms the other across all three surveys.

T_{PC1} vs Latitude		Second-order polynomial model		Two-segment piecewise linear model with break at latitude:					
				43.8º		45.4º		46.3º	
	Survey	AICc	AICc-Wt	AICc	AICc-Wt	AICc	AICc-Wt	AICc	AICc-Wt
	HS	93.94	0.15	98.43	0.02	91.32	0.54	92.54	0.29
	R1	94.58	0.08	100.49	0.00	94.26	0.09	89.94	0.82
	R2	95.63	0.10	101.32	0.01	96.18	0.08	91.51	0.81
Ch_{PC1} vs Latitude		Second-order polynomial model		Two-segment piecewise linear model with break at latitude:					
				43.8º		45.4º		46.3º	
	Survey	AICc	AICc-Wt	AICc	AICc-Wt	AICc	AICc-Wt	AICc	AICc-Wt
	HS	3.28	0.75	6.86	0.13	8.71	0.05	7.99	0.07
	R1	2.95	0.30	7.98	0.02	6.56	0.05	1.45	0.63
	R2	4.16	0.62	6.29	0.21	7.68	0.11	8.66	0.06
Ch_{PC1} vs T_{PC1}		Second-order polynomial model		Two-segment piecewise linear model with break at T_{PC1}:					
				-16.48		-0.61		1.28	
	Survey	AICc	AICc-Wt	AICc	AICc-Wt	AICc	AICc-Wt	AICc	AICc-Wt
	HS	3.71	0.60	12.02	0.01	5.86	0.20	6.00	0.19
				-5.81		2.99		10.01	
	R1	-13.78	0.30	-2.53	0.00	-6.23	0.01	-15.44	0.69
				-0.77		5.79		12.37	
	R2	-2.05	0.01	10.78	0.00	1.33	0.00	-11.42	0.99

Supplementary Table 4 | Summary of two-segment piecewise regression models for the relationship between T_{PC1} and latitude with breakpoint at 46.3º. ANOVA $F_{[3,8]}$ tests of overall model fit were significant at $P < 0.0001$ in all cases. Letters '*a*' and '*b*' denote slope and intercept, and subindices '1' and '2' denote < 46.3º and ≥ 46.3º latitude segments, respectively. All *P* values from Student's t-tests are two-tailed.

T_{PC1} vs Latitude					
Survey		*Coef.*	*SE*	*t*	*P*
HS	a_1	-5.147	0.736	-6.990	0.0001
	b_1	223.743	30.383	7.364	0.0001
	a_2	-1.217	1.164	-1.045	0.3264
	b_2	29.809	57.524	0.518	0.6183
	dif. (a_1-a_2)	-3.930	1.377	-2.853	0.0214
	dif. (b_1-b_2)	193.934	65.055	2.981	0.0176
R1	a_1	-4.916	0.661	-7.440	0.0001
	b_1	221.558	27.267	8.126	0.0000
	a_2	-1.223	1.045	-1.171	0.2753
	b_2	34.310	51.263	0.665	0.5250
	dif. (a_1-a_2)	-3.693	1.236	-2.988	0.0174
	dif. (b_1-b_2)	187.248	58.381	3.207	0.0125
R2	a_1	-4.616	0.705	-6.545	0.0002
	b_1	212.407	29.101	7.299	0.0001
	a_2	-0.429	1.115	-0.385	0.7103
	b_2	2.282	55.096	0.041	0.9680
	dif. (a_1-a_2)	-4.187	1.319	-3.174	0.0131
	dif. (b_1-b_2)	210.125	62.310	3.372	0.0098

Supplementary Table 5 | One-tailed exact Wilcoxon signed rank tests for positive paired differences in T_{PC1} and Ch_{PC1} between surveys (n = 12), and two-tailed exact independent samples Mann-Whitney U tests for differences in magnitude of HS to R1 shift and R1 to R2 shift between Mediterranean and temperate samples (n = 6).

Test	Comparison	T_{PC1}	Ch_{PC1}
Wilcoxon	HS vs R1	0.000	0.002
	R1 vs R2	0.000	0.005
Mann-Whitney U	Mediterranean vs temperate (R1 minus HS)	0.589	0.699
	Mediterranean vs temperate (R2 minus R1)	0.015	0.015

Supplementary Table 6 | Summary of second-order polynomial models for the relationships between Ch_{PC1} and latitude and Ch_{PC1} and T_{PC1}. ANOVA $F_{[2,9]}$ tests of overall model fit were significant at $P < 0.0001$ in all cases. Letters '*a*' and '*b*' indicate first- and second-order coefficients, respectively, and "*c*" denotes intercept. All *P* values from Student's t-tests are two-tailed.

Ch_{PC1} vs Latitude					
Survey		*Coef.*	*SE*	*t*	*P*
HS	*a*	-0.787	0.185	-4.253	0.0021
	b	0.007	0.002	3.553	0.0062
	c	20.084	4.083	4.916	0.0008
R1	*a*	-0.715	0.182	-3.920	0.0035
	b	0.007	0.002	3.286	0.0095
	c	18.343	4.026	4.556	0.0014
R2	*a*	-0.900	0.192	-4.690	0.0011
	b	0.009	0.002	4.164	0.0024
	c	22.256	4.237	5.248	0.0005
Ch_{PC1} vs T_{PC1}					
HS	*a*	0.028	0.002	-1.744	0.0000
	b	0.000	0.000	12.562	0.0634
	c	-0.161	0.093	2.117	0.1151
R1	*a*	0.002	0.001	20.960	0.0053
	b	0.000	0.000	4.162	0.0000
	c	-0.017	0.045	-3.657	0.0025
R2	*a*	0.014	0.003	5.588	0.0003
	b	0.000	0.000	4.349	0.0019
	c	-0.210	0.071	-2.954	0.0161

Supplementary Table 7 | Summary of second-order polynomial models for the relationships between Ch_{PC1} and the extreme temperature indices TXx_{PC1} and TXx_{PC1}. ANOVA $F_{[2,9]}$ tests of overall model fit were significant at $P < 0.0001$ in all cases. Letters '*a*' and '*b*' indicate first- and second-order coefficients, respectively, and "*c*" denotes intercept. All *P* values from Student's t-tests are two-tailed.

Ch_{PC1} vs TXx_{PC1}					
Survey		*Coef.*	*SE*	*t*	*P*
HS	*a*	0.032	0.003	13.051	0.0000
	b	0.000	0.000	1.984	0.0785
	c	-0.084	0.082	-1.033	0.3284
R1	*a*	0.026	0.002	11.214	0.0000
	b	0.000	0.000	3.072	0.0133
	c	-0.185	0.073	-2.513	0.0332
R2	*a*	0.018	0.002	9.178	0.0000
	b	0.001	0.000	6.102	0.0001
	c	-0.019	0.048	-3.882	0.0037
Ch_{PC1} vs TNn_{PC1}					
HS	*a*	0.021	0.001	15.931	0.0000
	b	0.000	0.000	1.679	0.1274
	c	-0.016	0.073	-2.257	0.0504
R1	*a*	0.019	0.002	11.464	0.0000
	b	0.000	0.000	1.849	0.0975
	c	-0.013	0.086	-1.489	0.1707
R2	*a*	0.013	0.003	4.240	0.0022
	b	0.000	0.000	2.743	0.0227
	c	-0.143	0.095	-1.510	0.1654

Supplementary Table 8 | One-way ANOVA F tests for the fit of second-order polynomial models to the relationship between chromosome (Ch_{PC1}) and extreme temperature indices (TXx_{PC1} and TNn_{PC1}) in comparison to simple linear models (Supplementary Figure 1), and Akaike Information Criterion with small-sample correction (AICc) and Akaike weights (AICc-Wt) for the relative fit of the TXx_{PC1} and TNn_{PC1} second-order polynomial models to the Ch_{PC1} data. The temperature index that better describes the chromosome data shifted from extreme minimum in the HS survey (AICc-Wt = 0.96) to extreme maximum in the R2 survey (AICc-Wt = 1.00). Adj. r^2 are adjusted r^2 values for second-order polynomial models; n= 12).

	Ch_{PC1} vs TXx_{PC1}					Ch_{PC1} vs TNn_{PC1}				
Survey	Adj. r^2	$F_{[9,1]}$	P	AICc	AICc-Wt	Adj. r^2	$F_{[9,1]}$	P	AICc	AICc-Wt
HS	0.939	3.936	0.079	2.81	0.04	0.964	2.821	0.127	-3.59	0.96
R1	0.931	9.439	0.013	2.03	0.27	0.941	3.418	0.098	-0.13	0.73
R2	0.963	37.230	0.000	-7.51	1.00	0.896	7.524	0.023	5.00	0.00